Technical Note: Introduction of a Superconducting Gravimeter as Novel Hydrological Sensor for the Alpine Research Catchment Zugspitze

Christian Voigt[1], Karsten Schulz[2], Franziska Koch[2], Karl-Friedrich Wetzel[3], Ludger Timmen[4], Till Rehm[5], Hartmut Pflug[1], Nico Stolarczuk[1], Christoph Förste[1] and Frank Flechtner[1,6]

1 GFZ German Research Centre for Geosciences, Section 1.2 Global Geomonitoring and Gravity Field, Telegrafenberg, 14473 Potsdam, Germany
2 Institute for Hydrology and Water Management, University of Natural Resources and Life Sciences (BOKU), Muthgasse 18, 1190 Vienna, Austria
3 Institute of Geography, Augsburg University, Alter Postweg 118, 86159 Augsburg, Germany
4 Institute of Geodesy, Leibniz University Hannover (LUH), Schneiderberg 50, 30167 Hannover, Germany
5 Environmental Research Station Schneefernerhaus (UFS), Zugspitze 5, 82475 Zugspitze, Germany
6 Institute of Geodesy and Geoinformation Science, Technische Universität Berlin (TUB), Kaiserin-Augusta-Allee 104-106, 10553 Berlin, Germany

Correspondence to: Christian Voigt (christian.voigt@gfz-potsdam.de)

Abstract. The Zugspitze Geodynamic Observatory Germany has been set up with a worldwide unique installation of a superconducting gravimeter at the summit of Mount Zugspitze on top of the well-instrumented high-alpine Partnach spring catchment being regarded as natural lysimeter. This karstic high-alpine site is largely dominated by a large mean annual precipitation of 2080 mm and a long seasonal snow cover period of 9 months with significant importance for water supply to its forelands, while it shows a high sensitivity to climate change. However, regarding the majority of alpine regions worldwide there is only weak knowledge on temporal water storage variations due to only sparsely distributed hydrological and meteorological point sensors and the large variability and complexity of signals in alpine terrain. This underlines the importance of well-equipped areas such as Mount Zugspitze serving as natural test laboratories for an improved monitoring, understanding and prediction of alpine hydrological processes. The observatory superconducting gravimeter OSG 052 supplements the existing sensor network as a novel hydrological sensor system for the direct observation of the integral gravity effect of total water storage variations in the alpine research catchment Zugspitze. Besides the experimental setup and the available datasets, the gravimetric methods based on the first 27 months of observations are presented. The snowpack is identified as primary contributor to seasonal water storage variations and thus to the gravity residuals with a signal range of up to 750 nm/s² corresponding to 1957 mm snow water equivalent measured at a representative station at the end of May 2019. First hydro-gravimetric sensitivity analysis are based on simplified assumptions of the snowpack distribution within the area around Mount Zugspitze. These reveal a snow-gravimetric footprint of up to 4 km distance around the gravimeter with a dominant gravity contribution from the snowpack in the Partnach spring catchment. This shows that the hydro-gravimetric approach can deliver important and representative integral insights into this high-alpine site. This work is regarded as a concept

study showing preliminary gravimetric results and sensitivity analysis for upcoming long-term hydro-gravimetric research projects.

1 Introduction

One of the grand societal challenges is ensuring a sufficient water supply under climate change conditions. The European Alps are of crucial importance to supply water for ecological, energy and societal purposes and with a relatively large fraction of annual precipitation received and stored, they are often referred to as water towers (Immerzeel et al., 2020; Beniston et al., 2018; Viviroli et al., 2007). The IPCC (2014) indicates that "in many regions, changing precipitation or melting snow and ice are altering hydrological systems, affecting water resources in terms of quantity and quality", thereby emphasizing the need for efficient future water management strategies, even in currently water secure regions (Immerzeel et al., 2020). To develop such strategies, a comprehensive understanding and quantification of changing hydrological processes in mountainous regions, including short- and long-term observations and model predictions are urgently required.

However, due to the high installation and maintenance costs of monitoring equipment, and often harsh environmental conditions causing instrument failure and difficult accessibility, hydro-meteorological observatories and subsequent data for high-alpine catchments are scarce. The Partnach spring catchment (Figure 1) in the southeast of the summit of Mount Zugspitze, also known as the Research Catchment Zugspitze (RCZ), covers an area of about 11 km² located in the Northern Limestone Alps and is one of the best-instrumented high-alpine catchments for monitoring snow hydrological processes (Bernhardt et al., 2018). Its main characteristics are a mean annual precipitation of 2080 mm with 80 % as snowfall from autumn to late spring above approx. 1800 m and an average temperature of -4.5°C regarding the climatic reference period 1981 to 2010 (Weber et al., 2016). The altitudes vary between 2962 m (summit of Mount Zugspitze) and 1430 m at Partnach spring. Due to a special geological karst situation, the entire catchment is solely drained by the Partnach spring, and can therefore be regarded as a natural lysimeter, allowing for detailed water balance and water movement studies (Wetzel, 2004; Rappl et al., 2010). Given this unique geological situation and the available instrumentation, the RCZ is part of the GEWEX International Network of Alpine Research Catchments (INARCH; Pomeroy et al., 2015). Germany's highest glacier remains - the Northern and Southern Schneeferner – are also located in the RCZ (Hagg et al., 2012) as well as permafrost in the rock walls of Mount Zugspitze (Krautblatter et al., 2010). The RCZ is part of the Bockhütte catchment with an area of 25 km². The Hammersbach catchment covers an area of 14 km² in northeastern direction from Mount Zugspitze and includes the Höllentalferner glacier. Karst hydrological characteristics can be found in Lauber and Goldscheider (2014).
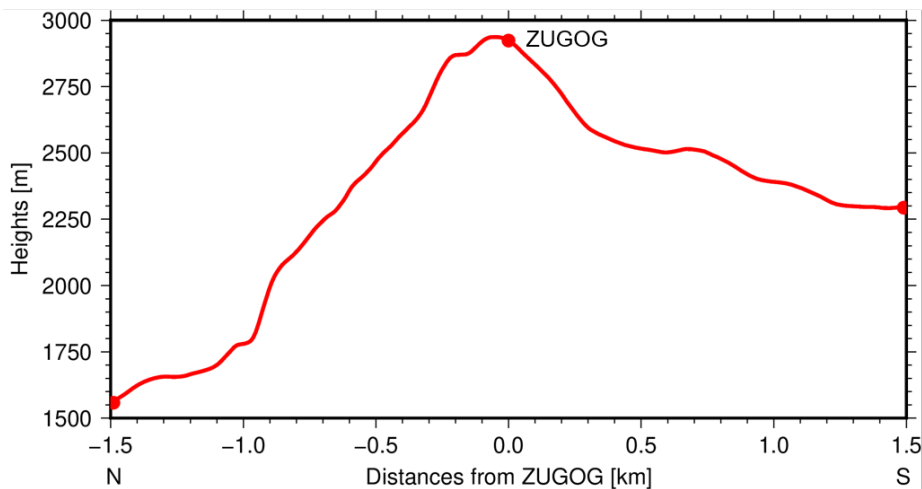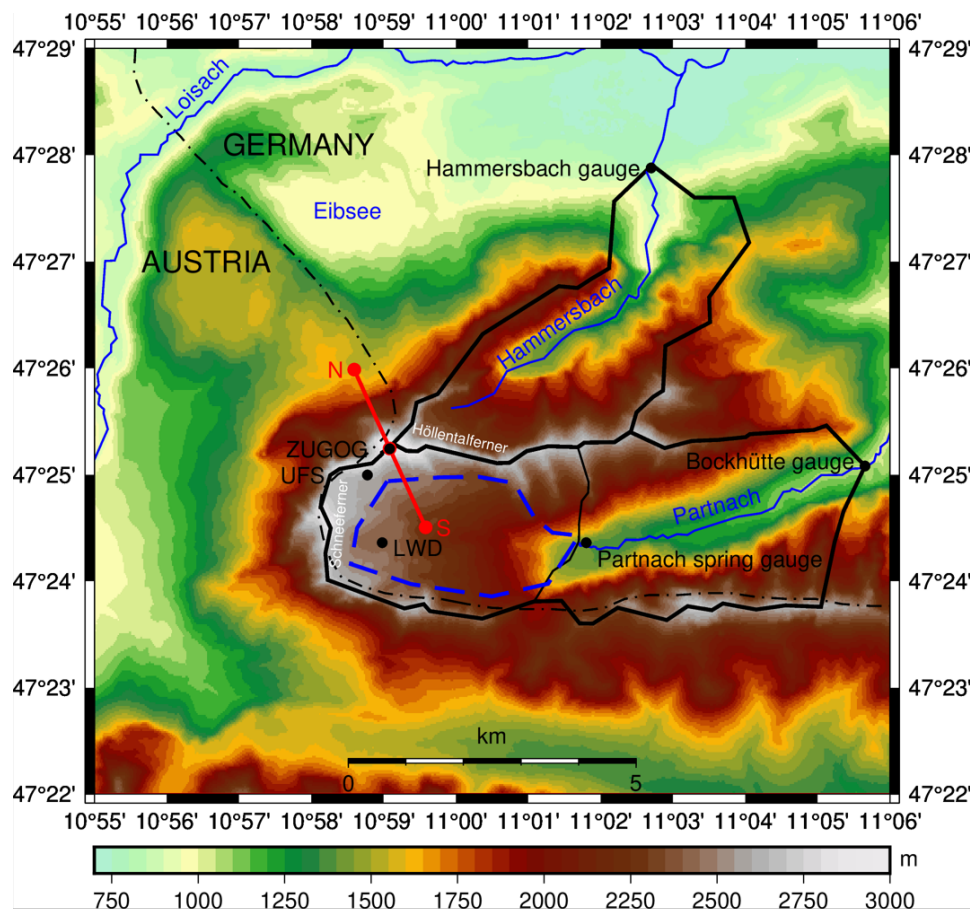
Figure 1: Topographic heights around the Zugspitze Geodynamic Observatory Germany (ZUGOG), the Environmental Research Station (UFS) and the hydro-meteorological station (LWD), the alpine catchments (white lines) Partnach spring (11 km²) as part of Bockhütte (25 km²) with their corresponding gauge stations as well as the Hammersbach catchment (14 km²) with its planned gauge station, and the estimated groundwater body below Zugspitzplatt (blue dashed line) as well as a topographic profile North-South profile through ZUGOG transverse to the maximum slopes (red line)

70

The environmental research station Schneefernerhaus (UFS), located in the RCZ, is easily accessible with cable cars, and operates a dense hydro-meteorological sensor network jointly with the German Weather Service (DWD) and the Bavarian Avalanche Warning Service (LWD) including a portable LiDAR sensor for spatially distributed snow height monitoring.

75 Detailed water balance and karst water discharge studies at the Partnach spring have investigated runoff responses to rainfall and snowmelt dynamics and characterized the karst groundwater aquifer (Hürkamp et al., 2019; Morche and Schmidt, 2012; Rappl et al., 2010; Wetzel, 2004). Numerous snow-hydrological studies investigated the spatiotemporal dynamics of snow cover and the snow water equivalent (SWE) (Bernhardt et al., 2018), combining monitoring techniques, such as terrestrial photogrammetry (Härer et al., 2013 and 2016), remote sensing (Härer et al., 2018) or LiDAR observations (Weber et al., 2016,

80 2020, and 2020a) with different complex snow-hydrological modelling. Some limitations arising from these studies were the small number of cloud-free remote sensing scenes in the visible and near-infrared spectrum to derive spatially distributed snow cover maps at high temporal resolutions, and the limited spatial extent of the terrestrial photogrammetry and LiDAR observations in the RCZ (Härer et al., 2016; Weber et al., 2016, and 2020). Both, photogrammetry and LiDAR observation techniques are only capable of measuring snow heights but not hydrologically relevant SWE values directly and thus rely on

85 additional snow density data from local snow pit or snow weight measurements. While snow cover and snow height data are able to condition the snow-hydrological model behaviour to some degree (Weber et al., 2020a), it has recently been shown that integral data from satellite (Bahrami et al., 2020) and terrestrial gravimetry (Güntner et al., 2017) providing footprint averaged time series of terrestrial water storage anomaly (TWSA) can greatly improve the identification of water balance components and relevant hydrological processes on catchment scale.

90

The last years of terrestrial gravimetric research have seen a transformation of superconducting gravimeter (SG) installations from low noise sites for the analysis of global geophysical phenomena to specific sites of interest for the monitoring of near-surface mass transport processes. These include the development of SGs as hydrological sensors for the direct, integral and non-invasive monitoring of water storage variations in a minimized field enclosure near Tucson, Arizona, USA (Kennedy et

95 al., 2014) and at Wettzell, Germany (Güntner et al., 2017) as well as SG installations for the monitoring of karst hydrological processes at the Larzac plateau, France (Fores et al., 2017), and at Rochefort, Belgium (Watlet et al., 2020). Creutzfeldt et al. (2013) use SG measurements at Wettzell, Germany, for the estimation of storage-discharge-relationships in a small headwater catchment. Very recently, Chaffaut et al. (2020) have reported about an SG installation at the summit of the Strengbach catchment in the French Vosges for the analysis of water storage dynamics. In this catchment, however, seasonal snow cover

100 only plays a minor role. In addition, SGs are applied in connection with absolute gravimeters (AGs) and relative spring gravimeters (RGs) in hybrid approaches for hydro-gravimetry (Naujoks et al., 2010), volcano monitoring (Carbone et al., 2019) and geothermal mass movements (Schäfer et al., 2020). These hybrid approaches exploit the advantages of the various types of gravimeters with the AGs providing long-term gravity changes, SGs for the continuous high-precision temporal gravity changes at the measurement sites and RGs for additional spatiotemporal variations in the area of interest (Hinderer et al., 2015).

105

Gravimetric methods are already applied in the RCZ. Episodic AG observations have been carried out since 2004 with a FG5 absolute gravity meter by the Leibniz University Hannover (LUH) for the analysis of long-term gravity changes at Mount Zugspitze and for a long-range gravimeter calibration base (Timmen et al., 2006; Peters et al., 2009). Timmen et al. (2021) estimate a geophysical trend of -20 nm/s²/yr with an uncertainty of 3 nm/s²/yr (single standard deviation 1σ) from AG observations between 2004 and 2019 as a consequence of alpine mountain uplift and hydrological mass loss. Monthly RG observations have been done with a transportable spring gravimeter since 2014 by the Technical University of Munich (TUM) for the analysis of periodic permafrost changes and cavity detection in a tunnel (Kammstollen) of Mount Zugspitze (Scandroglio et al., 2019). The most important gap in the hybrid gravimetric approach has now been closed by the installation of the SG at the summit of Mount Zugspitze enabling the separation of short-term, seasonal, interannual and long-term gravity changes.

The overall research question to be discussed in this study is to what extent the OSG 052 can contribute to a better understanding of hydrological processes in high-alpine catchments. This addresses the benefits and improvements of the hydro-gravimetric approach but also its challenges and limitations. After a presentation of the available data sets from gravimetry to hydrology and meteorology in the RCZ (section 2), the applied gravimetric methods for the separation of the hydrological signal from the gravity observations are shown (section 3). Section 4 contains the hydro-gravimetric results and sensitivity analysis with regard to various water storage components. Section 5 summarizes the main results and provides an outlook on future hydro-gravimetric projects.

2 Observations

2.1 The Zugspitze Geodynamic Observatory Germany

The Zugspitze Geodynamic Observatory Germany (ZUGOG) has been set up by the German Research Centre for Geosciences (GFZ) at the summit of Mount Zugspitze, Germany's highest mountain with an altitude of 2962 m, in a former laboratory of the Max Planck Institute for Extraterrestrial Physics (MPE), which was built in 1963 for the observation of cosmic rays (Figure 2). The 10 m high tower-like aluminium structure of the lab with an area of approx. 50 m² has a very steep roof to keep it free from snow. In addition, the position at the summit prevents hydrological mass variations above the sensor and simultaneously increases the hydro-gravimetric footprint (see also Chaffaut et al., 2020). Inside the lab, there is a measuring room with two concrete piers on the ground floor. While the first concrete pier is occupied by the SG, the second one is intended for absolute and relative gravimeters as well as other instruments. On the first floor are basic sleeping facilities for overnight stays if necessary. A ventilation reduces the heat produced by the compressor of the SG. This is necessary as the lab itself heats up considerably during sunny days. In addition, a thermally insulated box around the SG includes heaters to keep the sensor at a stable ambient temperature of around 25°C (±1°C). Temperature and humidity sensors have been installed in the lab. The power supplies of all electronics and compressor are secured by uninterruptible power supplies (UPS). The lab is accessible

all year round with cable cars from Germany and Austria. The UFS provides personnel and technical support as well as infrastructure during maintenance trips.

140

In September 2017, the OSG 052 was warmed up to room temperature at its former location in Sutherland, South Africa, and sent to the manufacturer GWR Instruments, Inc. in San Diego for maintenance after observing in parallel with the dual sphere OSG D-037 between 2008 and 2017 (Förste et al., 2016). This included refurbishment of the thermal levellers, an upgrade of the electronics from version GEP-2 to GEP-3, a modification of the dewar to enable cooling from room temperature down to

145 4 K with the accompanying refrigeration system, a replacement of the GPS antenna and a barometer specifically calibrated for a working altitude of 3000 m as well as an Intel mini Personal Computer for the operation of the UIPC software under Windows 7. After returning to GFZ, the OSG 052 has been moved to ZUGOG in September 2018 by truck, cogwheel train and helicopter at operating temperatures of 4 K. The first weeks of gravity observations with the OSG 052 showed an instrumental malfunction with a very large negative drift of about -50 nm/s²/day and several small offsets (cf. Schäfer et al., 2020). At the

150 end of October 2018, the instrument was warmed then re-cooled after abnormal drift was observed. The manufacturer (GWR) now recommends that SGs be transported at room temperature, and the dewar be evacuated just prior to cooling with the refrigeration system. According to GWR, development is currently in progress to eliminate these requirements.

The OSG 052 has been in nominal operation since 29 December 2018. ZUGOG is part of the International Geodynamics and

155 Earth Service (IGETS; Boy et al., 2020) providing Level 1 raw gravity and atmospheric pressure data with sampling rates of 1 s and 1 minute (Voigt et al., 2019) on a regular basis to the publicly accessible IGETS data base hosted by GFZ (Voigt et al., 2016). In addition, the continuous Global Navigation Satellite Systems (GNSS) station ZUGG (Ramatschi et al., 2019) is in operation since 9 Sep 2018 nearby the lab for the monitoring of surface displacements (Figure 2a). Several environmental sensors monitor local hydrological and meteorological variations. A snow scale and three laser-based snow height sensors

160 quantify the accumulated snow masses on the horizontal plane in front of the lab during the winter months (Figure 2c). After the experiences from the first winter 2018/2019, the pole with the snow height sensors had to be extended from 2.5 to 4 m. Another laser-based snow height sensor has a view to the slope directly below the SG. Laser-based sensors have been preferred instead of the widely used ultrasonic sensors because the snow cover is not horizontal. A small meteorological station outside the lab observes temperature and humidity as well as wind speed and direction. All data sets are part of a remotely controlled

165 monitoring system.

170

Figure 2: (a) The Zugspitze Geodynamic Observatory Germany (ZUGOG) with GNSS station in front; (b) OSG 052 installed on the ground floor at ZUGOG, (c) ZUGOG with snow height sensors and snow scale in front; (d) ZUGOG with a winter view of a part of the alpine research catchment Zugspitze including the Northern and Southern Schneeferner glaciers.

2.2 Hydrological and meteorological datasets in the research catchment Zugspitze

ZUGOG is connected to the UFS as the home base of a large research consortium operating a dense hydrological and meteorological sensor network for more than 20 years. Long-term meteorological datasets since 1900 are available on hourly to yearly basis from the Climate Data Center (CDC) of DWD for the station at the summit of Mount Zugspitze (Station ID 5792) including relative humidity, air temperature, precipitation height and form, wind speed and direction and air pressure. LWD provides several hydrological and meteorological datasets from a station at the Zugspitzplatt at an altitude of 2420 m including the SWE of the snowpack recorded by a snow scale. Moreover, in the last few years three further meteorological

stations were set up at the Zugspitzplatt as well as on two mountain ridges in the frame of the Virtual Alpine Observatory project (VAO).

Gauge stations monitor the discharge at Partnach spring and Bockhütte (Figure 1), while another gauge station is planned for the Hammersbach catchment. However, massive snowfall and corresponding spring discharge in spring 2019 have severely damaged the gauge station at Partnach spring and the data for the year 2019 is completely missing. A workaround has been installed in the spring of 2020 and a comprehensive maintenance of the whole station is scheduled for the summer of 2021.

The datasets are compiled in the Alpine Environmental Data Analysis Center (AlpEnDAC) as part of the VAO. Overall, this high-alpine region has one of the highest densities of meteorological stations worldwide and serves therefore as an ideal reference for testing new measurement and modelling approaches.

3 Gravimetric methodology

3.1 Pre-processing and calibration

The essential prerequisite for the application of the OSG 052 as a hydrological sensor is the separation of the hydrological signal from raw gravity observations. The required steps are explained for the period from 29 Dec 2018 to 31 Mar 2021 (27 months of observation). Raw gravity observations are voltage variations in 1 s sampling along with the observed barometric pressure variations and stored in daily files of the Tsoft format (Van Camp et al., 2005). These are compiled into monthly files and converted into the GGP format of IGETS (Voigt et al., 2016). Short data gaps up to 10 s are interpolated linearly on the full signal. For the decimation from 1 s to 1 min sampling, a double precision Chebyshev filter "g1s1m" with a filter length of 1009 s is applied (Crossley, 2010). For the reduction of the gravity data and the removal of spikes and offsets as well as the filling of longer gaps, the programs DETIDE and DESPIKE of ETERNA 3.4 (Wenzel, 1997) are used. Besides some steps on 7 Jan 2019 during the final centering of the sphere, the time series has shown only two additional steps on 24 Oct 2019 during a simulated power failure for UPS testing and on 7 Dec 2020 after exchanging the CMOS battery on the GEP remote card, which are eliminated manually with the program Tsoft. Finally, the monthly files in 1 min sampling are further decimated to one long time series in 1 h sampling by the program DECIMATE using symmetrical numerical FIR lowpass filters "N2H1M001" and "N14H5M01" from ETERNA 3.4.

For the transition from voltage to gravity variations, the amplitude factor of the OSG 052 is estimated on the basis of two absolute gravimeters and one calibrated spring gravimeter (Table 1). The first estimation was done in 2011 at Sutherland with FG5-301 by the German Federal Agency for Cartography and Geodesy (BKG). In order to validate this result after repeated transport of the SG and refurbishment at GWR, the second estimation was done in Sep 2018 at ZUGOG with FG5X-220 by LUH (Timmen et al., 2021), however, with a reduced accuracy due to the malfunction of the SG at this time (see section 2.1).

215 Hence, a third estimation was carried out over 4 weeks in Sep and Oct 2019 at ZUGOG on the basis of the relative spring gravimeter CG6-69 of GFZ calibrated in the gravimeter calibration system Hannover (Timmen et al., 2020). Within a least-squares adjustment, the amplitude factor of OSG 052 and a best-fitting polynomial reflecting the irregular drift of the CG6 are determined. The best fitting solution (smallest standard deviation for the amplitude factor) is found to be for blocks of 3 days, polynomials of degree 3 and 50 % overlap. The final amplitude factor is -749.59 nm/s²/V (1σ=0.22 nm/s²/V) as a weighted

220 mean from calibrations 1-3. The achieved accuracy is sufficient with regard to gravity residuals with a range of 750 nm/s² (Figure 3g), as amplitude factor deviations of 1 nm/s²/V correspond to maximum deviations of 1 nm/s² in gravity residuals, which can be used as measure for the accuracy of the gravity observations at ZUGOG.

The time delay of the OSG 052 is determined within a step response experiment developed by GWR on 1 March 2019 at

225 ZUGOG. 16 introduced step voltages are analysed with the program ETSTEP of ETERNA 3.4 (Wenzel, 1997) and the time delay is estimated to 10.53 s (1σ=0.03 s).

Table 1: Amplitude factors of the OSG 052 estimated from three calibrations

No of calibration	Method	Site	Period	Amplitude factor [nm/s²/V]	1σ uncertainty [nm/s²/V]
1	FG5-301 (BKG)	Sutherland	23-26 Nov 2011	-748.3	0.5
2	FG5X-220 (LUH)	Zugspitze	15-20 Oct 2018	-746.68	1.30
3	CG6-69 (GFZ)	Zugspitze	27 Sep-24 Oct 2019	-750.03	0.25
Mean value				-749.59	0.22

230 The instrumental drift of the OSG 052 is estimated to -20 nm/s²/yr based on two absolute measurements with FG5X-220 by LUH at 26-27 Sep 2019 and 30-31 Mar 2021 with 2477 and 5166 drops, respectively (Figure 3g). With regard to the uncertainty of 10-20 nm/s² (1σ) for the absolute measurements and the knowledge that the SG drift should be small and linear towards increasing gravity, the null hypothesis for the drift cannot be disproved statistically and no drift is applied within the subsequent analysis. Further absolute measurements planned for the future will increase the redundancy of the drift estimation and longer

235 temporal differences between the absolute measurements will make the drift estimation more robust. Unfortunately, the first absolute measurements from 15-20 Oct 2018 cannot be used as additional reference value for the drift estimation, as the SG had to be warmed up and cooled again for re-initialisation at the end of Dec 2018 (section 2.1), so that there is no connection to the current continuous SG time series.

3.2 Tidal analysis

240 In order to reduce the gravity effects from solid Earth and ocean tides, a local tidal model is computed based on 2 years of observations (29 Dec 2018 – 31 Dec 2020) with the program ANALYZE of ETERNA 3.4 (Wenzel, 1997) for the analysis of monthly, diurnal, semidiurnal and shorter tidal waves. The estimated amplitude factors and phase leads according to the

ETERNA wave grouping for a 1-year gravity time series are displayed in Table 2. The numerical high-pass filtering and a Hann window usually applied for the analysis of diurnal and semi-diurnal waves are deactivated for the simultaneous analysis of the monthly waves resulting in higher standard deviations for the shorter waves. Instead, a Chebyshev polynomial of degree 2 is applied in order to eliminate any long-term instrumental trend signal or long-term variations in gravity. Longer tidal waves (half year periods and longer) are considered by nominal values, i.e. amplitude factors of 1.16 and phases of 0°. Along with the tidal waves, the single admittance factor between gravity and barometric pressure is determined with -3.6506 nm/s²/hPa (1σ=0.0393 nm/s²/hPa). In order to reduce the large seasonal gravity signal, a second admittance factor is determined between gravity and the snow water equivalent (SWE) with 0.2965 nm/s²/mm (1σ=0.0007 nm/s²/mm; cf. section 4.2). The gravity variations induced by solid Earth and ocean tides are predicted with the local tidal parameters from Table 2 and shown for the analysed period in Figure 3b.

3.3 Non-tidal gravity reductions

Besides tidal variations, the gravity observations include significant non-tidal effects shown in Figure 3. For a more detailed compilation of temporal gravity field variations see e.g. Voigt et al. (2016a), while Mikolaj et al. (2019) quantify time-domain uncertainties for the different gravity reductions. The signal admittance factor from the tidal analysis of -3.6506 nm/s²/hPa includes the maximum correlated signal between observed gravity and barometric pressure. For a refined modelling of gravity variations induced by mass redistributions in the atmosphere, the Atmospheric attraction computation service (Atmacs; Klügel and Wziontek, 2009) provides effects from local to global scales with a temporal resolution of 3 h based on 3D ECMWF weather data. However, the limited spatial resolution of the weather models of 7 km for Europe shows that the complex topography around the station cannot be represented sufficiently. In order to account for the limited spatial resolution and to improve the temporal resolution, the following procedure is used. The gravity observations are reduced by the effects of solid Earth and ocean tides, Earth rotation and SWE variations as well as regional and global atmospheric effects from Atmacs. In this way, the gravity residuals primarily reflect the effects of local atmospheric mass redistributions. The admittance factor between these gravity residuals and the observed barometric pressure variations is estimated to -2.9190 nm/s²/hPa (1σ=0.0274). For the total atmospheric reduction, the local part of Atmacs is replaced by this admittance factor multiplied by the observed pressure variations in 1 h sampling and added to the regional and global atmospheric effects from Atmacs (Figure 3c).

Table 2: Estimated amplitude factors and phase leads from a least-squares adjustment of 23 tidal waves based on 2 years of gravity observations with OSG 052 at ZUGOG

Frequencies [cpd]		Wave	Theoretical Amp.[nm/s²]	Amplitude factor	Std	Phase lead [°]	Std [°]
from	to						
0.020885	0.054747	MM	21.1656	1.01201	0.18789	9.1622	10.6146
0.054748	0.091348	MF	40.0581	1.11718	0.04843	5.8775	2.4845
0.091349	0.122801	MTM	7.6699	1.42938	0.16566	-6.1562	6.6347
0.122802	0.501369	MQM	1.2250	1.24028	0.60193	5.1859	27.8178
0.501370	0.911390	Q1	59.3059	1.14954	0.00152	-0.1425	0.0756
0.911391	0.947991	O1	309.7475	1.15060	0.00031	0.0454	0.0154
0.947992	0.981854	NO1	24.3484	1.14980	0.00302	0.3313	0.1505
0.981855	0.998631	P1	144.1019	1.15094	0.00066	0.0240	0.0327
0.998632	1.001369	S1	3.4048	1.38514	0.03875	23.9574	1.6028
1.001370	1.023622	K1	435.4574	1.13835	0.00022	0.1490	0.0110
1.023623	1.035379	TET1	4.6578	1.15618	0.02065	1.1388	1.0233
1.035380	1.057485	J1	24.3569	1.15438	0.00384	0.0779	0.1905
1.057486	1.071833	SO1	4.0394	1.13676	0.02372	0.9770	1.1951
1.071834	1.470243	OO1	13.3201	1.15354	0.00642	0.1334	0.3188
1.470244	1.880264	2N2	10.5279	1.15943	0.00249	2.4868	0.1229
1.880265	1.914128	N2	65.9181	1.17379	0.00053	2.0941	0.0260
1.914129	1.950419	M2	344.2804	1.18640	0.00011	1.5090	0.0052
1.950420	1.984282	L2	9.7321	1.17467	0.00407	1.7836	0.1984
1.984283	2.002736	S2	160.1632	1.18501	0.00023	0.1346	0.0112
2.002737	2.451943	K2	43.5108	1.18753	0.00087	0.4461	0.0422
2.451944	3.381378	M3	4.5825	1.07740	0.00484	-0.0481	0.2573
3.381379	4.347615	M4	0.0566	0.25408	0.25504	95.3389	57.5061
4.347616	7.000000	M5	0.0007	29.93575	20.46948	30.4792	39.1786

280

Temporal variations of the Earth's rotation vector with respect to the Earth's body are described by the pole coordinates and the Earth rotation angle and provided as Earth orientation parameters (EOP) by the International Earth Rotation and Reference Systems Service (IERS). For the computation of the thereby induced gravity variations, the program PREDICT of ETERNA 3.4 (Wenzel, 1997) is applied with the long term file EOP 14 C04 (IAU1980) provided by the International Earth Rotation and

285 Reference Systems Service (IERS) and amplitude factors set to 1.16 considering the elastic properties of a deformable solid Earth (Figure 3d).

Non-tidal ocean loading at Mount Zugspitze is caused by the attraction of non-tidal water mass variations in the Atlantic Ocean and the Mediterranean Sea and the vertical displacement of the Earth's crust due to the loading of these water masses. For the

290 computation of these small effects with a range of 5 nm/s², the Matlab toolbox mGlobe v1.1.0 (Mikolaj et al., 2016) is applied on the basis of 3-hourly total ocean bottom pressure anomalies (dataset "oba") from the GRACE Atmosphere and Ocean De-aliasing Level-1B (AOD1B RL06) products (Dobslaw et al., 2017) and shown in Figure 3e.

Hydrological gravity variations can be subdivided into those from local scales (up to several meters around the gravimeter)
over alpine catchment scales (from several meters to kilometers) to non-local scales (from several kilometers). Non-local
hydrological gravity variations include both attraction effects and surface loading, while for local to catchment scales only the
attraction effects from mass redistributions are considered. Non-local hydrological effects are provided by the EOST Loading
Service (Boy, 2021) using, e.g., the Modern-Era Retrospective analysis for Research and Applications, Version 2 (MERRA-
2; Gelaro et al., 2017) with spatial resolutions of 0.5° and 0.625° in latitude and longitude, respectively, and 1 h temporal
resampling. These effects are displayed in Figure 3f.

Figure 3 shows the process of signal separation from gravity observations of OSG 052 to gravity residuals by reducing all
shown and explained effects for the period from 29 Dec 2018 to 31 Mar 2021. These gravity residuals are the primary target
signal for hydro-gravimetric studies at Mount Zugspitze reflecting predominantly total water storage variations on different
scales. An exceptionally large seasonal gravity range of up to 750 nm/s² is visible compared to other SG installations in Central
Europe with seasonal variations of approx. 100 nm/s² range (Abe et al., 2012). However, it should also be noted that the gravity
residuals also include uncertainties in the model-based signal separation, which are typically at the level of a few nm/s² root-
mean-square error (Mikolaj et al., 2019). In addition, non-hydrological signals from alpine geological mass redistributions are
also included in the gravity residuals. Typical examples are avalanches, rockfalls and landslides occurring on time scales from
seconds to days. Regular controlled avalanche blasting with an impact of approx. -5 nm/s² on the gravity signal have already
been noticed. On long time scales, the impact of mountain uplift and its separation from climate-driven long-term hydrological
variations must be considered (Timmen et al., 2021).

An important task is the reduction of local hydrological signals in order to enhance the sensitivity towards the catchment scale.
While the steep roof of the lab and its position above the slope at the summit are very advantageous, most of the disturbing
signals are expected from snow masses on a horizontal plane with an area of 5 m x 10 m directly in front of the lab (Figure 2c)
where a local snow monitoring network has been set up. Here, considerable amounts of snow accumulate during the winter
due to precipitation, drift of snow and snow cleared of a nearby visitors platform with a snow blower. A first estimation of the
maximum signal from snow heights of 4 m and densities of 300 kg/m³ reveals a significant gravity effect of 25 nm/s²
superimposed by somewhat smaller event-like signals during heavy snowfall events. As this is only a fraction of 1:30 with
regard to the total gravity residual range and due to initial problems as a consequence of very harsh conditions during winter
2018/19 (frozen snow height sensors, torn cables, too low sensor pole height), a model-based description of the local snowpack
situation has not yet been set up completely.
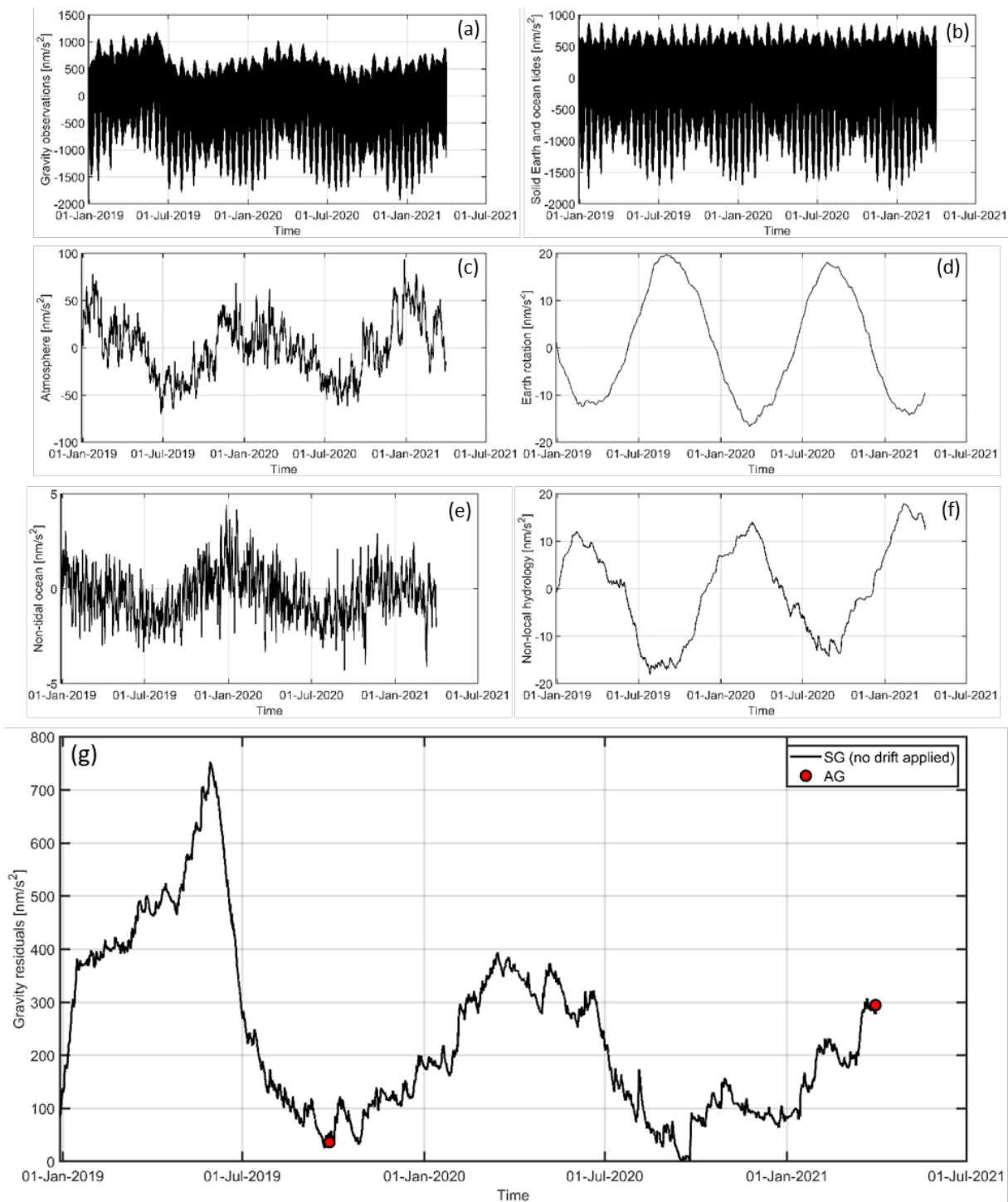
Figure 3: Signal separation from gravity observations (a) to gravity residuals (g) including two absolute measurements (red circles) by reducing gravity variations induced by solid Earth and ocean tides (b), atmospheric mass redistributions (c), Earth rotation (d), non-tidal ocean (e) and non-local hydrological mass redistributions (f). Please note the different scaling of the axes.

330

4 Hydro-gravimetric results and sensitivity analysis

4.1 Water balance

The subsequent hydro-gravimetric analysis based on the gravity residuals from Figure 3g focus, for the first time, on a high-alpine region largely dominated by seasonal snow cover. The gravity residuals reflect the total water storage variations from local to catchment scales as the balance of precipitation, glacial melt, retention in the karst, spring discharge and evapotranspiration. As the large complexity and variability of the hydrological parameters make the hydrological modelling very difficult, continuous gravity observations providing the integral signal of all mass redistributions in the vicinity of the gravimeter should thus be highly beneficial serving as constrains for the hydrological modelling on catchment scale.

From the first 27 months of observations, the high interannual variability of water storage maxima can be determined with 752 nm/s² at 29 May 2019 and 393 nm/s² at 14 Mar 2020 significantly differing in time of year and in amplitude by a factor of two due to seasonal snowpack variations. The seasonal minima, however, are very close in time and amplitude with a difference of -24 nm/s² between 16 Sep 2020 and 21 Sep 2019, respectively, fitting very well with the estimated trend of -20 nm/s²/yr estimated from absolute gravity observations between 2004 and 2019 by Timmen et al. (2021). They suggest that the main contribution is caused by glacier diminishing, and a smaller part is explained by mountain uplift (1 mm causes -2 nm/s²). With a multi-year continuous gravity time series from OSG 052, it is possible to study the evolution of seasonal and - in combination with absolute gravity observations - also long-term water storage variations.

However, for the hydrological decomposition of the gravity residuals into individual water storage components, complementary data from meteorological and hydrological techniques are needed. According to Newton's law of gravitation, the gravimetric method is known to be most sensitive to local mass variations with a signal attenuation by 1/r² (r being the distance between gravimeter and source mass). As gravimeters are solely sensitive in vertical direction, attenuations occur for mass variations towards horizontal direction (see also Creutzfeldt et al., 2008). Hence, the essential question is how sensitive the gravity residuals are with regard to individual water storage components from local to catchment scales. This question will be addressed in the following sections.

4.2 Snowpack

Representative observations of the snow water equivalent (SWE) for the Zugspitzplatt are available from the LWD station (Figure 1). The spatiotemporal variations of the snowpack around the summit of Mount Zugspitze are the main contributors to the gravity residuals from autumn to spring. Figure 4 shows the gravity residuals, the SWE multiplied by the estimated regression factor between gravity residuals and SWE of 0.298 nm/s²/mm (1σ = 0.003 nm/s²/mm). The high correlation of 0.963 between the gravity residuals and SWE (sample size 19771) is clearly visible and both are following similar seasonal patterns.

In general, the winter seasons of 2018/19 and 2019/20 were very different. The first winter season is characterized by a sharp increase in SWE of approx. 300 nm/s² in mid-January as well as in the second half of May due to massive snowfall. The maximum SWE is extraordinary high, with a value of 1957 mm measured at the LWD station, compared to an annual mean of the maximum SWE at approx. 1350 mm since the installation of the snow scale in 2014 until now. Contrary, the second winter season with a maximum SWE of 1147 mm at the LWD station represents a winter with a small to normal amount of snow. While in 2019 the seasonal gravity and SWE maxima coincide at 29 May, there is a difference of more than one month between gravity and SWE maxima in 2020, i.e. 14 Mar and 19 Apr, respectively. However, in 2020 there was no distinctive SWE peak rather a longer period with maximal SWE values between these two dates. Higher temperatures during April 2020 led to an early onset of snowmelt in the lower part of the catchment with beginning recharge of the karst water body and increasing spring discharge at Partnach spring.

Despite the high correlation between gravity and SWE from the LWD station at Zugspitzplatt, there are still significant additional signals remaining with a range of 250 nm/s². The reasons are quite manifold. First, the single point observations of the SWE at LWD station are not fully representative for the large variations of the snowpack and its distribution at catchment scale particularly considering the altitude and temperature gradient within the area. During periods of massive snowfall this leads to remaining signals of up to 150 nm/s². Moreover, rain events during the short summer season cause rapid gravity increases of up to 100 nm/s² followed by an equally fast but only partial decrease and a slower subsequent decline due to the lagged drainage back to the gravity level before the specific rain event (Timmen et al., 2021). Second, signals from other water storage components are not considered within the regression analysis with the major remaining signals of up to 200 nm/s² occurring during the main melting periods and corresponding spring discharge from May to July and additional signals of up to 100 nm/s² during the short snow free summer season (Figure 6).

Sensitivity analysis of a simple snowpack distribution assumption in the surroundings are carried out exemplarily for the times of maximum seasonal gravity residuals at 29 May 2019 and 14 Mar 2020. In order to take into account the topography for the spatial snow distribution, the high-resolution digital terrain model DGM50/M745 by BKG from 2006 with a grid spacing of 1" x 1" (20 m longitude x 30 m latitude) is used. Following assumptions are made for the snowpack distribution at the specific dates:

1. Computing the gravity effect from topography by integration of all rectangular prisms of 20 m x 30 m areas and constant heights.
2. Initially putting a homogeneous snowpack of maximum SWE of 1957 mm and 1075 mm, respectively, on top of every rectangular prism for the topography.
3. Linearly decreasing the snowpack on slopes with a value of 50 % at 45° slope and 0 % at 90° slope.

Further linearly decreasing the snowpack for lower elevations between 2000 and 1500 m with 0 % snowpack at 1500 m (only valid for the late spring of the examples).

Figure 5 shows the assumed spatial distribution of the snowpack around Mount Zugspitze at 29 May 2019 and 14 Mar 2020 (a and c, respectively) and the cumulative snow-gravimetric sensitivities with regard to the ZUGOG gravimeter site (b and d, respectively) with the essential results summarised in Table 3. The assumed snow distributions provide gravity values of 764 nm/s² (752 nm/s² observed) and 420 nm/s² (393 nm/s² observed), respectively, for the two dates corresponding to deviations of 2 % and 6 %. The gravity contributions from all areas coloured from deep red to yellow in Figures 5b and d are defined as snow-gravimetric footprint with contributions of 99.87 % (29 May 2019) and 99.76 % (14 Mar 2020), respectively, omitting residuals of 1 nm/s² of the total signal.
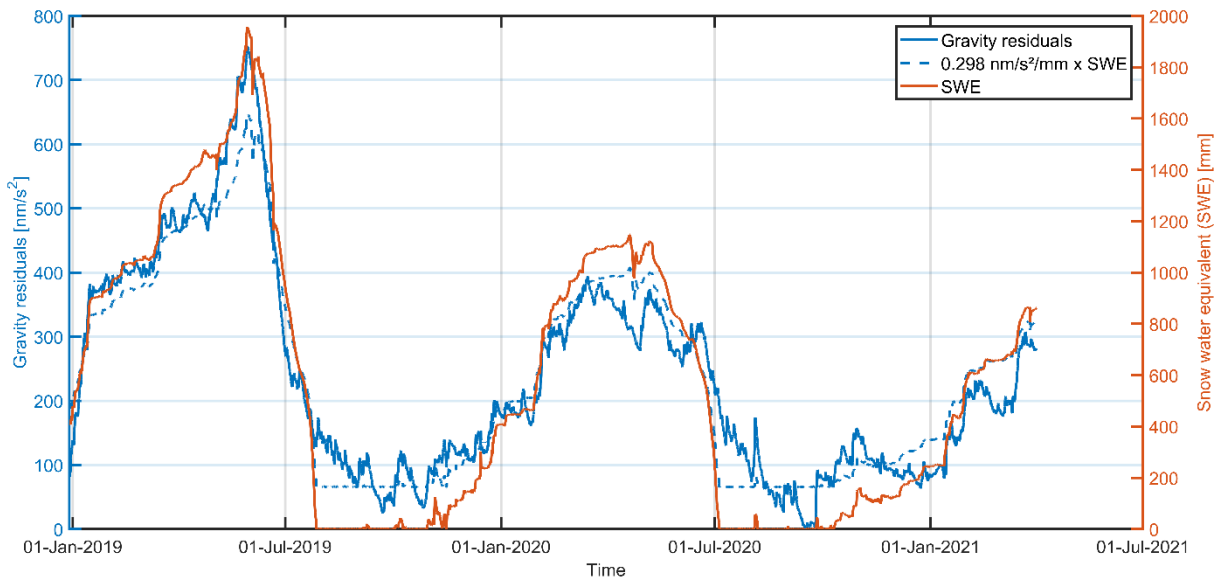
Figure 4: Gravity residuals (solid blue), snow water equivalent (solid red) from LWD station at Zugspitzplatt and SWE multiplied with the estimated regression factor of 0.298 nm/s²/mm between gravity residuals and snow water equivalent (dashed blue line)

The results show that the gravimeter observations are sensitive to the snowpack on catchment scales up to 3.5 km horizontal and 4 km slant distances to the gravimeter with a resulting snow-gravimetric footprint of approx. 40 km² (Figure 5). The major contribution comes from prisms in the RCZ with 71 % in both examples. The Hammersbach catchment has a much less significant contribution of 6 % only, as this lies on the opposite side of Mount Zugspitze and has very steep slopes near the summit. The additional gravity contribution from the snowpack in the remaining eastern parts of the Bockhütte catchment is negligible. The assumed spatial distribution of the snowpack suggests that the remaining 23 % contribution to the total gravity signal come from snow masses of the nearby summit area northwest from ZUGOG. These effects in the close vicinity should

be much smaller in reality compared to our very simple assumption of snow distribution, as the maximum snowpack at the summit is certainly less than the values from the LWD station due to usually strong winds at the summit ridge, which are neglected up to this point. Also the topography to the north-west of ZUGOG is very steep, in parts vertical, which allows for less snow accumulation and frequent discharge in the form of avalanches. Still, the local snowpack distribution in the direct vicinity of the SG needs special attention due to artificial snow accumulations around the summit. This knowledge will improve the snow-gravimetric sensitivities towards catchment scales.

4.3 Karst groundwater and spring discharge

Besides snow distribution and snow water equivalent, the liquid water balance in the karstified RCZ is influencing the SG signal. Throughout the year, a typical course of spring discharge with four characteristic periods can be observed at the Partnach spring gauge (Figure 6). From the end of October to April no recharge of the karst system takes place and the Partnach spring is falling dry. With rising temperatures in April, melting processes are beginning in the lower parts of the catchment and first meltwater pulses can be observed at the Partnach river gauge. Melting period in the upper part of RCZ starts later in May lasting until the beginning of July. The karst system of RCZ is mainly fed by meltwater and discharge at the Partnach spring is continuously high. Liquid precipitation leads to pronounced spring discharge peaks on top of the increased basal discharge level. During this period of time, spring discharge at the Partnach spring is a mixture of meltwater from areas with increasing elevations and liquid precipitation. After melting ends, long lasting rainfall and storm precipitation are dominating spring discharge characteristics with steep rising and falling limbs. The well-developed karst system of RCZ with conduit flow causes these rapid spring discharge reactions of the Partnach spring. With lowering temperatures during autumn, snow accumulation starts in higher elevations of RCZ and recharge of karst groundwater is reduced because liquid precipitation is more seldom. Sometimes daily melting cycles of the glacier remains of Northern and Southern Schneeferner can be observed during this usually dry period. At the end of autumn, low temperatures and snowfall in higher elevations are terminating recharge and karst groundwater head is falling step by step beneath the level of the Partnach spring.
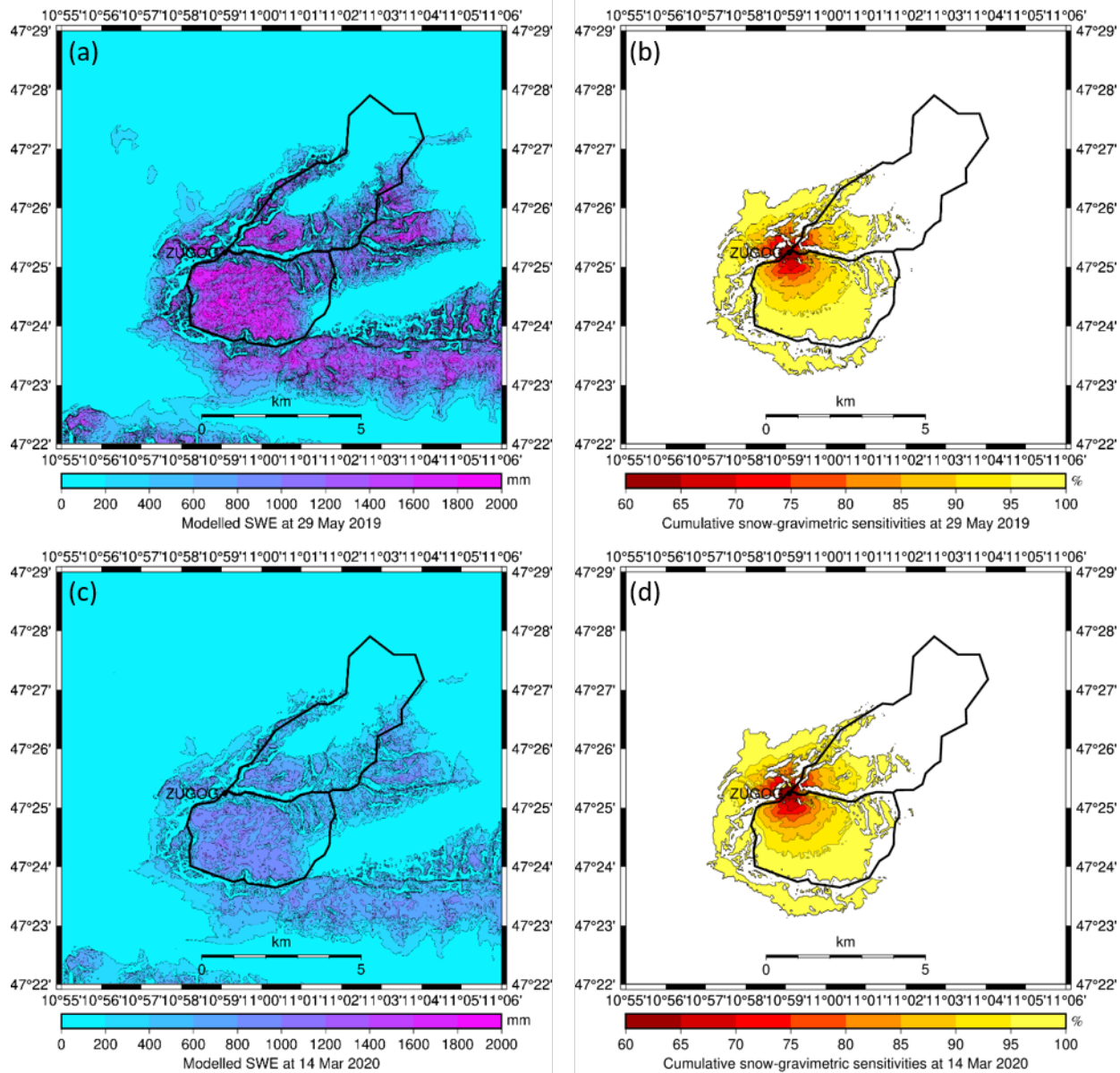
Figure 5: Estimated SWE of the snowpack at maximum seasonal gravity residuals (a and c) and corresponding cumulative snow-gravimetric sensitivities (b and d) with regard to ZUGOG at 29 May 2019 and 14 Mar 2020, respectively. The boundaries of the Partnach spring and Hammersbach catchments are shown as black line. Sensitivities are shown only up to 99.87% and 99.76%, respectively, for the given examples, omitting residuals of 1 nm/s² of the total signal.

445

Table 3: Gravity contributions from modelled snowpack of various areas with regard to ZUGOG at maximum seasonal gravity residuals at 29 May 2019 and 14 Mar 2020

	29 May 2019		14 Mar 2020	
Area	Δg [nm/s²]	Δg [%]	Δg [nm/s²]	Δg [%]
Total	763.9	100.0	420.4	100.0
Snow-gravimetric footprint (deep red to yellow areas in Figure 5)	762.9	99.9	419.4	99.8
Partnach spring catchment (RCZ)	542.0	71.0	297.6	70.8
Hammersbach catchment	46.3	6.1	25.5	6.1
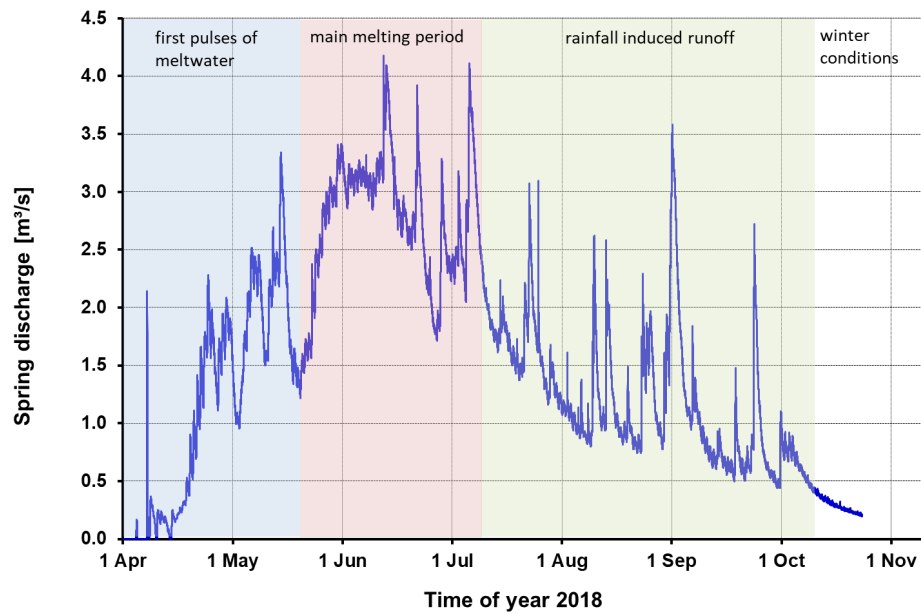
Figure 6: Spring discharge characteristics of the Partnach spring during 2018.

During seasonal snowmelt periods in spring and especially after the snowpack has fully disappeared in summer, other signals become the main contributors to the water storage variations observed by the gravimeter. The largest part of the melting snow fills the vadose zone of the karstified underground body down to an altitude of 1440 m below the Zugspitzplatt (Figure 1). If the groundwater level is rising with beginning recharge of the vadose zone, the spring discharge starts at the Partnach spring which is usually well observed by a gauge station. Unfortunately, the spring discharge data is not available for 2019 (section 2.2). From the seasonal gravity minima at 21 Sep 2019 and 16 Sep 2020, respectively, being very close in time despite the very different snow masses, a large variability in the spring discharge processes as a consequence of the seasonal snowpack can be stated.

For the hydrological interpretation of gravity signals from ZUGOG, it is crucial to quantify the water volume stored in the vadose karst zone of RCZ. Thereto, pseudo-continuous depletion curves are constructed by splicing short falling hydrograph

465 intervals together (e.g. Lamb and Beven, 1997). The recession constant "α" is calculated for several years, because recession behaviour of the Partnach spring varies from year to year due to unknown processes in the karst system (Figure 7a). Based on a mean recession constant "α", a water storage model for the vadose karst zone is developed by an addition of daily discharge volumes during the depletion period. As Figure 7b shows, storage volume in the vadose zone varies between 1.6 and 3.38 x 10^6 m³. Under the assumption of a homogeneous layer of a 6 km² wide groundwater body (Figure 1), these numbers correspond

470 to water level changes of 0.27 and 0.56 m, respectively, that can be translated to groundwater level changes depending on the aquifer porosity. Sensitivity analysis with regard to the ZUGOG site reveal corresponding gravity values between 12 and 24 nm/s², respectively. With an uncertainty of a few nm/s², the gravimetric approach should be able to distinguish interannual groundwater height variations.

475 Besides seasonal spring discharge and corresponding karst groundwater variations, rainfall events on time scales from hours to days produce significant peak-like signals not only in the spring discharge but also in the gravimetric time series. A homogeneous layer of 1 mm precipitation height on top of the digital terrain model applied (section 4.2) result in a gravity increase of 0.9 nm/s². This shows that the gravity variations can be used as reference for the estimation of the total sum of precipitation (Delobbe et al., 2019) in this alpine terrain with large variability in precipitation instead of using point

480 measurements with precipitation collectors. The higher precipitation admittance factor (factor 3 compared to 0.298 nm/s²/mm for the SWE) results from the large geographical heterogeneity of the SWE in the RCZ. The SWE of the snowpack recorded by the snow scale at the LWD station provides maximum SWE values, while the precipitation height is set as a homogeneous layer.

485 The same hydro-gravimetric approach might be applied to the estimation of daily evapotranspiration rates (Van Camp et al., 2016) during dry days in late summer (August and September), when the seasonal spring discharge has mainly finished. In general, evapotranspiration is small in high-alpine areas, especially due to less available soil moisture in shallow alpine soils or even the absence of soils at all, sparse vegetation and less demand of plants and decreases with increasing altitude (Gurtz et al., 1999). Maximum evapotranspiration rates of 2-3 mm/day for high-alpine environments inducing gravity effects of 1.8 to

490 2.7 nm/s², respectively, at the ZUGOG gravimeter site are at the limit of what can be observed by the gravimeter.

Finally, glacier melting and permafrost degradation also contribute to groundwater and spring discharge with predominant climate-driven long-term signals but also significant interannual variations e.g. as a consequence of very dry and hot summers (Scandroglio et al., 2019). In addition, cavities inside Mount Zugspitze filled with water through permafrost degradation might

495 lead to disturbances of the gravimetric signal on catchment scale depending on the distance and direction to the gravimeter and their sizes. These additional signals will be best captured by the combination of absolute, superconducting and relative gravimetry and other geodetic techniques in a future hybrid approach. Thus, the whole summit area could be covered by a gravity network, constrained by the SG at ZUGOG, and observed regularly within episodic campaigns.

500
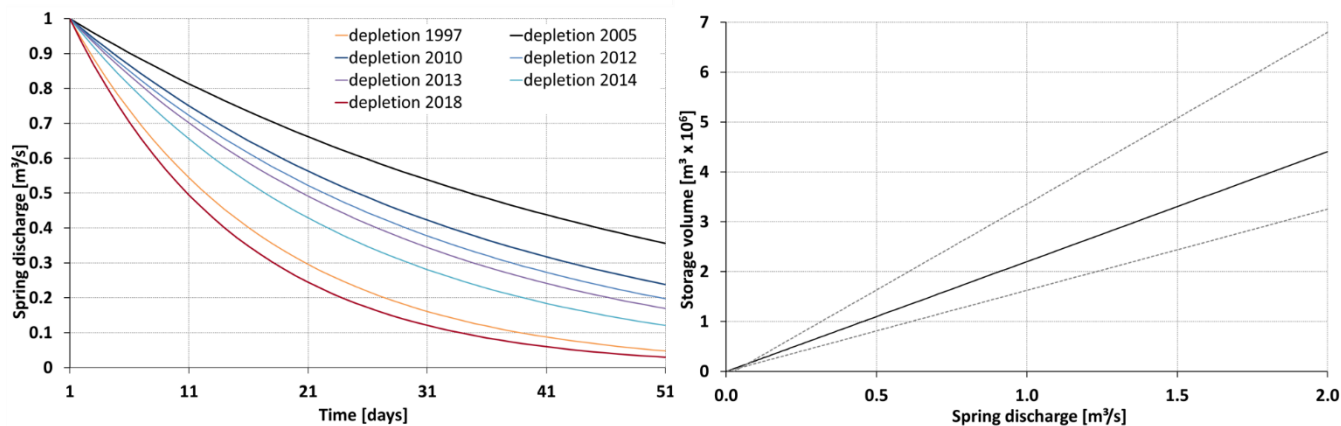
Figure 7: Depletion curves of the karst groundwater of RCZ for selected years (a) and calculated storage volumes of the groundwater body at different levels of spring discharge (b). The solid line shows the relationship for a mean recession constant "α" of 0.4 and the dashed lines are enclosing the range of one standard deviation.

5 Summary and conclusions

505   The superconducting gravimeter OSG 052 is introduced as a novel hydrological sensor for the direct observation of the integral gravity effect of total water storage variations in the high-alpine Partnach spring catchment (Research Catchment Zugspitze RCZ), and a high-quality and publicly available continuous gravity time series of 27 months is provided. The RCZ is among the best equipped high-alpine catchments with lysimeter characteristics and now supplemented by a superconducting gravimeter to address the complex hydrological situation, dominated by snow cover, melting glaciers and degrading permafrost

510   as well as karst groundwater.

Spatiotemporal variations of the snowpack are the main contributor to the gravity residuals. Sensitivity analysis on the basis of a simplified assumption on snow distribution in this area reveal a snow-gravimetric footprint of 3.5 km horizontal and 4 km slant distances around the gravimeter covering an area of 40 km². The large range of gravity residuals up to 750 nm/s²

515   corresponds to the maximum of 1957 mm snow water equivalent on 29th May 2019, measured at the LWD station located on the Zugspitzplatt. This result, together with the low uncertainty of the gravity residuals of a few nm/s², enables various detailed future hydro-gravimetric analysis as the snow masses from the RCZ contribute to more than 2/3 of the total gravity signal.

Based on this concept study, the description of the snowpack distribution will be refined in future studies for the entire

520   Zugspitze region and the three catchments Partnach spring, Bockhütte and Hammersbach. The aim is to set up snowpack models such as SNOWPACK/Alpine3D (Lehning et al., 2006) or use cold region hydrological model frames like the Canadian Hydrological Model (CHM, Marsh et al., 2020) at this location, and, in addition, to statistically describe the main snowpack

distribution via LiDAR measurements, similar as presented in Grünewald et al. (2013). With these approaches, the descriptions of the spatial snowpack distribution will be improved in this very complex high-alpine terrain by including detailed descriptions of the snowpack itself, the effect of energy balance on the snowpack, potential wind redistributions as well as further meteorological and gravimetrical influences on the snow cover regarding elevation, aspect and slope – and of course by using the gravity residuals as boundary conditions.

During the mainly snow-free season in summer, other water storage components dominate the gravity residuals. Spring discharge and karst groundwater variations are driven not only by snowmelt and rain but also by glacier melting and permafrost degradation. While the discharge of the Partnach spring and Bockhütte catchments are generally well observed by gauge stations, the estimation of catchment-wide total rainfall amounts and evapotranspiration rates will strongly benefit from including the gravity residuals into the analysis. The high-resolution model of the spatiotemporal variations of the snowpack amount and distribution will be coupled with a hydrological model to an efficient physically based, spatially distributed karst-snow-hydrological model describing relevant physical processes in the RCZ.

Further improvements and enhancements are also planned for the gravimetric part. The setup of a more detailed and small scale snowpack description, especially in the direct vicinity of the SG with artificial snow accumulations, is essential in order to increase the sensitivity towards the whole catchment. For this purpose, a high resolution DTM with a grid spacing of 1 m x 1 m will be used in the future in combination with a detailed 3D surveying of the buildings at the summit. With regard to atmospheric gravity effects, the complex alpine topography surrounding ZUGOG should be taken into account either by using a weather model with a higher spatial resolution or by setting up a local model based on an array of available barometers (Riccardi et al., 2007). Additional absolute gravity measurements will stabilize the SG drift estimation and support long-term studies, while the GNSS station nearby ZUGOG reveals the long-term vertical displacement of the site. It is further intended to install a continuously recording ZLS-Burris spring gravimeter in a vertical distance of 500 m below OSG 052 inside Mount Zugspitze in a technical room next to the rails of the cogwheel train to quantify the ongoing mass redistributions and time delays inside the mountain. In addition, the integration of episodic relative gravity measurements both from the tunnel of Mount Zugspitze and from the RCZ would be highly beneficial in a future hybrid gravimetric approach in order to better capture the spatiotemporal gravity variations on catchment scales – and with this for a more thorough constraining of the hydrological model.

The overall aim is an improved understanding and a better predictability of alpine mass redistributions on catchment scales which can be transferred to other alpine research catchments worldwide. Finally, an improved knowledge of hydrological variations on catchment scales enhances the resolution of large-scale hydrological variations and reduces the spatial and temporal gap to the satellite mission GRACE-FO (Gravity Recovery and Climate Experiment – Follow On), launched in May 2018, which provides gravity variations with a spatial resolution of 300 x 300 km² and a temporal resolution of 1 month.

Data availability

Raw gravity and atmospheric pressure data from the OSG 052 at ZUGOG are published (Voigt et al. 2019) and available from the IGETS data base hosted by the Information System and Data Center at GFZ (URL: https://isdc.gfz-potsdam.de/igets-data-base/). The subsequent gravity residuals and all auxiliary data from ZUGOG can be provided upon request from the author. Hydro- and meteorological datasets of the area around Mount Zugspitze and beyond are available from the Alpine Environmental Data Analysis Center (AlpEnDAC) as part of the VAO (URL: https://www.alpendac.eu).

Author contribution

CV: Conceptualization, Data curation, Formal analysis, Funding acquisition, Investigation, Methodology, Project administration, Visualization, Writing – original draft preparation, review & editing. **KS, FK, KFW:** Conceptualization, Investigation, Methodology, Writing – original draft preparation, review & editing. **LT:** Data curation, Formal analysis, Writing – review & editing. **TR:** Data curation, Project administration, Resources, Writing – review & editing. **HP, NS:** Data curation, Project administration, Writing – review & editing. **CF, FF:** Funding acquisition, Project administration, Resources, Writing – review & editing.

Competing interests

The authors declare that they have no conflict of interest.

Acknowledgements

The Generic Mapping Tools (GMT) have been used to prepare some figures. The Zugspitze Geodynamic Observatory Germany (ZUGOG) is part of the Modular Earth Science Infrastructure (MESI) of GFZ. We thank the staff of Umweltforschungsstation Schneefernerhaus, Deutsche Funkturm, Bayerische Zugspitzbahn and Tiroler Zugspitzbahn for their personnel and technical support. We also thank Pieter Fourie from the South African Astronomical Observatory (SAAO) for sharing his expertise from Sutherland with us during the installation of the SG at Mount Zugspitze. Bettina Schaefli, David Crossley and two anonymous reviewers are gratefully acknowledged for their constructive and valuable comments and improvements to the manuscript.

References

Bahrami, A., Goita, K., and Magagi, R.: Analysing the contribution of snow water equivalent to the terrestrial water storage over Canada, Hydrological Processes, 34, 175-188, doi:10.1002/hyp.13625, 2020.

Beniston, M., Farinotti, D., Stoffel, M., Andreassen, L. M., Coppola, E., Eckert, N., Fantini, A., Giacona, F., Hauck, C., Huss, M., Huwald, H., Lehning, M., López-Moreno, J.-I., Magnusson, J., Marty, C., Morán-Tejéda, E., Morin, S., Naaim, M., Provenzale, A., Rabatel, A., Six, D., Stötter, J., Strasser, U., Terzago, S., and Vincent, C.: The European mountain cryosphere: a review of its current state, trends, and future challenges, The Cryosphere, 12, 759–794, doi:10.5194/tc-12-759-2018, 2018.

Bernhardt, M., Härer, S., Feigl, M., and Schulz, K.: Der Wert Alpiner Forschungseinzugsgebiete im Bereich der Fernerkundung, der Schneedeckenmodellierung und der lokalen Klimamodellierung, Österr. Wasser- und Abfallw., 70, 515-528, doi:10.1007/s00506-018-0510-8, 2018.

Boy, J.-P.: EOST Loading Service, URL: http://loading.u-strasbg.fr, last accessed: 30 Apr 2021, 2021.

Boy, J.-P., Barriot, J.-P., Förste, C., Voigt, C., and Wziontek, H.: Achievements of the first 4 years of the International Geodynamics and Earth Tide Service (IGETS) 2015 – 2019, IAG Symp, doi: 10.1007/1345_2020_94, 2020.

Carbone, D., Cannavò, F., Greco, F., Reineman, R., and Warburton, R. J.: The Benefits of Using a Network of Superconducting Gravimeters to Monitor and Study Active Volcanoes, J. Geophys. Res.-Sol. Ea., 123, 2153-2165, doi:10.1029/2018JB017204, 2019.

Chaffaut, Q., Hinderer, J., Masson, F., Viville, D., Pasquet, S., Boy, J. P., Bernard, J. D., Lesparre, N., and Pierret, M. C.: New insights on water storage dynamics in a mountainous catchment from superconducting gravimetry, Geophys. J. Int. (submitted), 2020.

Creutzfeldt, B, Güntner, A., Klügel, T., and Wziontek, H.: Simulating the influence of water storage changes on the superconducting gravimeter of the Geodetic Observatory Wettzell, Germany, Geophysics, 73, doi:10.1190/1.2992508, 2008.

Creutzfeldt, B., Troch, P., Güntner, A., Ferré, T. P. A., Graeff, T., and Merz, B.: Storage-discharge relationships at different catchment scales based on local high-precision gravimetry. Hydrol. Process., 28, 1465–1475, doi:10.1002/hyp.9689, 2013.

Crossley, D.: GGP Decimation Filters, URL: http://www.eas.slu.edu/GGP/ggpfilters.html, created 27 Mar 2007, updated 19 Apr 2010, last access 11 Nov 2020, 2020.

Delobbe, L., Watlet, A., Wilfert, S., and Van Camp, M.: Exploring the use of underground gravity monitoring to evaluate radar estimates of heavy rainfall, Hydrol. Earth Syst. Sci., 23, 93-105, doi: 10.5194/hess-23-93-2019, 2019.

Dobslaw, H., Bergmann-Wolf, I., Dill, R., Poropat, L., Thomas, M., Dahle, C., Esselborn, S., König, R., and Flechtner, F.: A new high-resolution model of non-tidal atmosphere and ocean mass variability for de-aliasing of satellite gravity observations: AOD1B RL0,. Geophys. J. Int., 211, 263-269, doi:10.1093/gji/ggx302, 2017.

Fores, B., Champollion, C., Le Moigne, N., Bayer, R., and Chéry, J.: Assessing the precision of the iGrav superconducting gravimeter for hydrological models and karstic hydrological process identification. Geophys. J. Int., 208, 269–280, doi:10.1093/gji/ggw396, 2017.

Förste, C., Voigt, C., Abe, M., Kroner, C., Neumeyer, J., Pflug, H., and Fourie, P.: Superconducting Gravimeter Data from Sutherland - Level 1, GFZ Data Services, doi:10.5880/igets.su.l1.001, 2016.

Gelaro, R., McCarty, W., Suárez, M.J., Todling, R., Molod, A., Takacs, L., Randles, C.A., Darmenov, A., Bosilovich, M.G., Reichle. R., Wargan, K., Coy, L., Cullather, R., Draper, C., Akella, S., Buchard, V., Conaty, A., da Silva, A.M., Gu, W., Kim,

G.-K., Koster, R., Lucchesi, R., Merkova, D., Nielsen, J.E., Partyka, G., Pawson, S., Putman, W., Rienecker, M., Schubert, S.D., Sienkiewicz, M., and Zhao, B.: The Modern-Era Retrospective Analysis for Research and Applications, Version 2 (MERRA-2), J. Climate, 30, 5419-5454, doi:10.1175/JCLI-D-16-0758.1, 2017.

620 Grünewald, T., Stötter, J., Pomeroy, J. W., Dadic, R., Moreno Baños, I., Marturià, J., Spross, M., Hopkinson, C., Burlando, P., and Lehning, M.: Statistical modelling of the snow depth distribution in open alpine terrain, Hydro. Earth Syst. Sci., 17, 3005-3021, doi:10.5194/hess-17-3005-2013, 2013.

Güntner, A., Reich, M., Mikolaj, M., Creutzfeldt, B. Schröder, S., and Wziontek, H.: Landscape-scale water balance monitoring with an iGrav superconducting gravimeter in a field enclosure, Hydrol. Earth Syst. Sci., 21, 3167–3182, 625 doi:10.5194/hess-21-3167-2017, 2017.

Gurtz, J., Baltensweiler, A. and Lang, H.: Spatially distributed hydrotope-based modelling of evapotranspiration and runoff in mountainous basins. Hydrol. Process., 13, 2751-2768, doi:https://doi.org/10.1002/(SICI)1099-1085(19991215)13:17%3C2751::AID-HYP897%3E3.0.CO;2-O, 1999.

Hagg, W., Mayer, C., Mayr, E., and Heilig, A.: Climate and glacier fluctuations in the Bavarian Alps in the past 120 years, 630 Erdkunde, 66, 121-142, 2012.

Härer, S., Bernhardt, M., Corripio, J. G., and Schulz, K.: PRACTISE – Photo Rectification And ClassificaTIon SoftwarE (V.1.0), Geosci. Model Dev., 6, 837–848, doi:10.5194/gmd-6-837-2013, 2013.

Härer, S., Bernhardt, M., and Schulz, K.: PRACTISE – Photo Rectification And ClassificaTIon SoftwarE (V.2.1), Geosci. Model Dev., 9, 307–321, doi:10.5194/gmd-9-307-2016, 2016.

635 Härer, S., Bernhardt, M., Siebers, M., and Schulz, K.: On the need for a time- and location-dependent estimation of the NDSI threshold value for reducing existing uncertainties in snow cover maps at different scales, The Cryosphere, 12, 1629–1642, doi:10.5194/tc-12-1629-2018, 2018.

Hinderer, J., Crossley, D., and Warburton, R.: Superconducting Gravimetry, in: Treatise on Geophysics, 2nd edition, edited by: Gerald Schubert, Elsevier, Oxford, Vol 3., 59-115, doi:10.1016/B978-0-444-53802-4.00062-2 59, 2015.

640 Hürkamp, K., Zentner, N., Reckerth, A., Weishaupt, S., Wetzel, K.-F., Tschiersch, J., and Stumpp, C.: Spatial and temporal variability of snow isotopic composition on Mt. Zugspitze, Bavarian Alps, Germany, J. Hydrol. Hydromech., 67, 49–58, doi:10.2478/johh-2018-0019, 2019.

Immerzeel, W.W., Lutz, A.F., Andrade, M., Bahl, A., Biemans, H., Bolch, T., Hyde, S., Brumby, S., Davies, B.J., Elmore, A.C., Emmer, A., Feng, M., Fernández, A., Haritashya, U., Kargel, J.S., Koppes, M., Kraaijenbrink, P.D.A., Kulkarni, A.V., 645 Mayewski, P.A., Nepal, S., Pacheco, P., Painter, T.H., Pellicciotti, F., Rajaram, H., Rupper, S., Sinisalo, A., Shrestha, A.B., Viviroli, D., Wada, Y., Xiao, C., Yao, T., and Baillie, J. E. M.: Importance and vulnerability of the world's water towers, Nature, 577, 364-369, doi:10.1038/s41586-019-1822-y, 2020.

IPCC: Climate Change 2014: Synthesis Report. Contribution of Working Groups I, II and III to the Fifth Assessment Report of the Intergovernmental Panel on Climate Change [Core Writing Team, R.K. Pachauri and L.A. Meyer (eds.)], IPCC, Geneva, 650 Switzerland, 151 pp, 2014.

Kennedy, J., Ferré, T. P. A., Güntner, A., Abe, M., and Creutzfeldt, B.: Direct measurement of subsurface mass change using the variable baseline gravity gradient method, Geophys. Res. Lett., 41, doi:10.1002/2014GL059673, 2014.

Klügel, T., and Wziontek, H.: Correcting gravimeters and tiltmeters for atmospheric mass attraction using operational weather models, J. Geodyn., 48, 204-210, doi:10.1016/j.jog.2009.09.010, 2009.

655 Krautblatter, M., Verleysdonk, S., Flores-Orozco, A. and Kemna, A.: Temperature-calibrated imaging of seasonal changes in permafrost rock walls by quantitative electrical resistivity tomography (Zugspitze, German/Austrian Alps), J. Geophys. Res., 115, F02003, doi:10.1029/2008JF001209, 2010.

Lamb, R. and Beven, K.: Using interactive recession curve analysis to specify a general catchment storage model, Hydrol. Earth Syst. Sci., 1, 101– 113, doi:10.5194/hess-1-101-1997, 1997.

660 Lauber, U. and Goldscheider, N.: Use of artificial and natural tracers to assess groundwater transit-time distribution and flow systems in a high-alpine karst system (Wetterstein Mountains, Germany), Hydrogeology Journal, 22, 1807-1824, doi:10.1007/s10040-014-1173-6, 2014.

Lehning, M., Völksch, I., Gustafsson, D., Nguyen, T., Stähli, M., and Zappa, M.: ALPINE3D: A detailed model of mountain surface processes and its application to snow hydrology, Hydrological Processes, 20, 2111–2128, doi:10.1002/hyp.6204, 2006.

665 Marsh, C. B., Pomeroy, J. W., and Wheather, H. S.: The Canadian Hydrological Model (CHM) v1.0: a multi-scale, multi-extent, variable-complexity hydrological model – design and overview, Geosci. Model Dev., 13, 225–247, doi:10.5194/gmd-13-225-2020, 2020.

Mikolaj, M., Meurers, B., and Güntner, A.: Modelling of global mass effects in hydrology, atmosphere and oceans on surface gravity, Comput. Geosci., 93, 12–20, doi:10.1016/j.cageo.2016.04.014, 2016.

670 Mikolaj, M., Reich, M., and Güntner, A.: Resolving Geophysical Signals by Terrestrial Gravimetry: A Time Domain Assessment of the Correction-Induced Uncertainty, J. Geophys. Res.-Sol. Ea., 124, doi:10.1029/2018JB016682, 2019.

Morche, D., and Schmidt, K.-H.: Sediment transport in an alpine river before and after a dambreak flood event. Earth Surf. Process. Landforms, 37, 347–353, doi:10.1002/esp.2263, 2012.

Naujoks, M., Kroner, C., Weise, A., Jahr, T., Krause, P., and Eisner, S.: Evaluating local hydrological modelling by temporal 675 gravity observations and a gravimetric three-dimensional model, Geophys. J. Int., 182, 233–249, doi:10.1111/j.1365-246X.2010.04615.x, 2010.

Peters, T., Schmeer, M., Flury, J., and Ackermann, C.: Erfahrungen im Gravimeterkalibriersystem Zugspitze, zfv, 3/2019., 2009.

Pomeroy, J., Bernhardt, M., and Marks, D.: Research network to track alpine water, Nature, 521, doi:10.1038/521032c, 2015.

680 Ramatschi, M., Bradke, M., Nischan, T., and Männel, B.: GNSS data of the global GFZ tracking network, GFZ Data Services, doi:10.5880/GFZ.1.1.2020.001, 2019.

Rappl, A., Wetzel, K.-F., Büttner, G., and Scholz, M.: Tracerhydrologische Untersuchungen am Partnach-Ursprung, Hydrologie und Wasserbewirtschaftung, 54, 222-230, 2010.

Scandroglio, R., Heinze, M., Schröder, T., Pail, R., and Krautblatter, M.: A first attempt to reveal hydrostatic pressure in

685   permafrost-affected rockslopes with relative gravimetry, Geophysical Research Abstracts, 21, EGU2019-12870, 2019.

Riccardi, U., Hinderer, J., and Boy, J.-P.: On the efficiency of barometric arrays to improve the reduction of atmospheric effects on gravity data, Physics of the Earth and Planetary Interiors, 161, 224-242, doi:10.1016/j.pepi.2007.02.007, 2007.

Schäfer, F., Jousset, P., Güntner, A., Erbas, K., Hinderer, J., Rosat, S., Voigt, C., Schöne, T., and Warburton, R.: Performance of three iGrav superconducting gravity meters before and after transport to remote monitoring sites, Geophys. J. Int., 223, 959-

690   972, doi:10.1093/gji/ggaa359, 2020.

Timmen, L., Flury, J., Peters, T., and Gitlein, O.: A new absolute gravity base in the German Alps, M. Hvozdara and I. Kohuh (eds.): Contributions to Geophysics and Geodesy, Vol. 36, 2nd Workshop on International Gravity Field Research (special issue), 2006.

Timmen, L., Rothleitner, C., Reich, M., Schröder, S., and Cieslak, M.: Investigation of Scintrex CG-6 Gravimeters in the

695   Gravity Meter Calibration System Hannover, AVN, 127, 155-162, 2020.

Timmen, L., Gerlach, C., Rehm, T., Völksen, C., and Voigt, C.: Geodetic-gravimetric monitoring for mountain uplift and hydrological variations at Zugspitze and Wank, Remote Sens., 13, doi:10.3390/rs13050918, 2021.

Van Camp, M. and Vauterin, P.: Tsoft: graphical and interactive software for the analysis of time series and Earth tides, Comput. Geosci., 31, doi:10.1016/j.cageo.2004.11.015, 2005.

700   Van Camp, M., de Viron, O., Pajot-Métivier, G., Casenave, F., Watlet, A., Dassargues, A., and Vanclooster, M.: Direct measurement of evapotranspiration from a forest using a superconducting gravimeter, Geophys. Res. Lett., 43, 10,225-10,231, doi:10./1002/2016GL070534, 2016.

Viviroli, D., Dürr, H. H., Messerli, B., Meybeck, M., and Weingartner, R.: Mountains of the world, water towers for humanity: Typology, mapping, and global significance. Water Resour. Res., 43, doi:10.1029/2006WR005653, 2007.

705   Voigt, C., Förste, C., Wziontek, H., Crossley, D., Meurers, B., Palinkas, V., Hinderer, J., Boy, J.-P., Barriot, J.-P., and Sun, H.: Report on the data base of the international geodynamics and earth tide service (IGETS), Scientific technical report STR Potsdam, GFZ German Research Centre for Geosciences, doi:10.2312/gfz.b103-16087, 2016.

Voigt, C, Denker, H., and Timmen, L.: Time-variable gravity potential components for optical clock comparisons and the definition of international time scales, Metrologia, 53, 1365-1383, doi:10.1088/0026-1394/53/6/1365, 2016a.

710   Voigt, C., Pflug, H., Förste, C., Flechtner, F., and Rehm, T.: Superconducting Gravimeter Data from Zugspitze - Level 1, GFZ Data Services, doi:10.5880/igets.zu.l1.001, 2019.

Watlet A., Van Camp M., Francis O., Poulain A., Rochez G., Hallet V., Quinif Y., and Kaufmann O.: Gravity monitoring of underground flash flood events to study their impact on groundwater recharge and the distribution of karst voids, Water Resour. Res., 56, doi:10.1029/2019WR026673, 2020.

715   Weber, M., Bernhardt, M., Pomeroy, J. W., Fang, X., Härer, S., and Schulz, K.: Description of current and future snow processes in a small basin in the Bavarian Alps. Environ. Earth Sci., 75, 1223, doi:10.1007/s12665-016-6027-1, 2016.

Weber, M., Feigl, M., Schulz, K., and Bernhardt, M.: On the Ability of LIDAR Snow Depth Measurements to Determine or Evaluate the HRU Discretization in a Land Surface Model, Hydrology 7(2), 20, doi:10.3390/hydrology7020020, 2020.

720 Weber, M., Koch, F., Bernhardt, M., and Schulz, K.: The evaluation of the potential of global data products for snow hydrological modelling in ungauged high alpine catchments, Hydrol. Earth Syst. Sci. Discuss. [preprint], doi:10.5194/hess-2020-326, in review, 2020a.

Wenzel, H.-G.: ETERNA Version 3.40, Earth Tide Data Processing Package ETERNA, 1997.

Wetzel, K.-F.: On the hydrology of the Partnach area in the Wetterstein mountains (Bavarian Alps), Erdkunde, 58: 172-186, 2004.